The ion line intensities become too weak to be measured accurately when the temperatures drop to below 11000 K. This precludes using the ion-neutral pair for determining temperatures except near the jet axis. For this reason the temperature determined by the ion-neutral method is used as the reference temperature in equation (2). The final temperature distribution is then obtained by the method based on equation (2) which is useful out to the region where the temperature drops to 9000 K. This is the lower limit to which the assumption of thermodynamic equilibrium may still be applied.

Figures 1 and 2 show the change in radial temperature distribution for different currents. The mass flow rates given correspond to extreme operating conditions. The low mass flux case was not run at 200 A as was the high mass flux case since the stability here was too poor for spectrometric measurements. It is interesting to note the crossing of the profiles for the low mass flux case where the flow is laminar and presumably the arc column is very well defined. As the self-magnetic field is increased with increasing current, a certain radial pressure gradient is developed. This pressure gradient makes the actual arc radius smaller. This effect would not be so noticeable in the high mass flux case where the flow is turbulent and the turbulent diffusion of energy would be much more significant than retardation due to magnetic pressure on the column. The relative proximity of the 200 A and 400 A profiles for small radii in Fig. 2 is probably due to experimental errors since if one were to fit an appropriate second or third degree curve to the data, the curves would be somewhat further apart in the 1 mm region.

The temperature distributions as functions of radius and axial position are given as isotherms in Fig. 3 for the low mass flux jet and in Fig. 4 for the high mass flux turbulent jet. The current of 400 A was chosen for these measurements because the stability was best here for both cases and therefore the results would be more meaningful. The data for $z > 8$ mm in Fig. 3 are somewhat in doubt because of the low ion intensities at this distance

REFERENCES

1. W. FINKELNBURG and H. MAECKER, Elektrische Bogen und Thermisches Plasma, *Handb. Phys.* **22**, 254–444 (1956).
2. C. J. CREMERS and E. PFENDER, The thermal characteristics of a high and low mass flux plasma jet, USAF Office of Aerospace Research, ARL 64-191 (1964).

Int. J. Heat Mass Transfer Vol. 11, pp. 1206–1208 Pergamon Press 1968 Printed in Great Britain

PATTERNS OF FREE CONVECTION FLOW ADJACENT TO HORIZONTAL HEATED SURFACES

R. B. HUSAR and E. M. SPARROW
University of Minnesota, Minneapolis, Minnesota, U.S.A.

(*Received* 29 *January* 1968)

INTRODUCTION

THIS paper is concerned with the free convection flow field adjacent to horizontal, upward-facing heated surfaces having various planforms (square, rectangle, triangle, circle). A flow visualization technique is employed which is an extension of that described by Baker [1]. The fluid motions are made visible by local changes of color of the fluid itself, the color changes resulting from changes in pH (acidic to basic). The aim of the investigation is to provide insights into the nature of the free convection flow field, with particular emphasis on the influence of the shape of the heated surface which generates the flow.

Available experimental information on the heat-transfer characteristics of upward-facing heated surfaces is incomplete and somewhat contradictory. For square plates, McAdams [2], following Fishenden and Saunders [3], provides a correlating equation which differs from that of Mikheyev [4] by 30 per cent. The correlation of Bosworth [5] is in substantial agreement with Mikheyev's, provided that the characteristic dimensions in the respective correlating equations have the same meanings. Temperature and velocity field measurements [6, 7] have been made only for square plates. Information for surfaces other than squares is generally lacking. Flow visualization studies have, apparently, not heretofore been performed.

EXPERIMENTAL APPARATUS

The surfaces employed in the flow visualization studies are

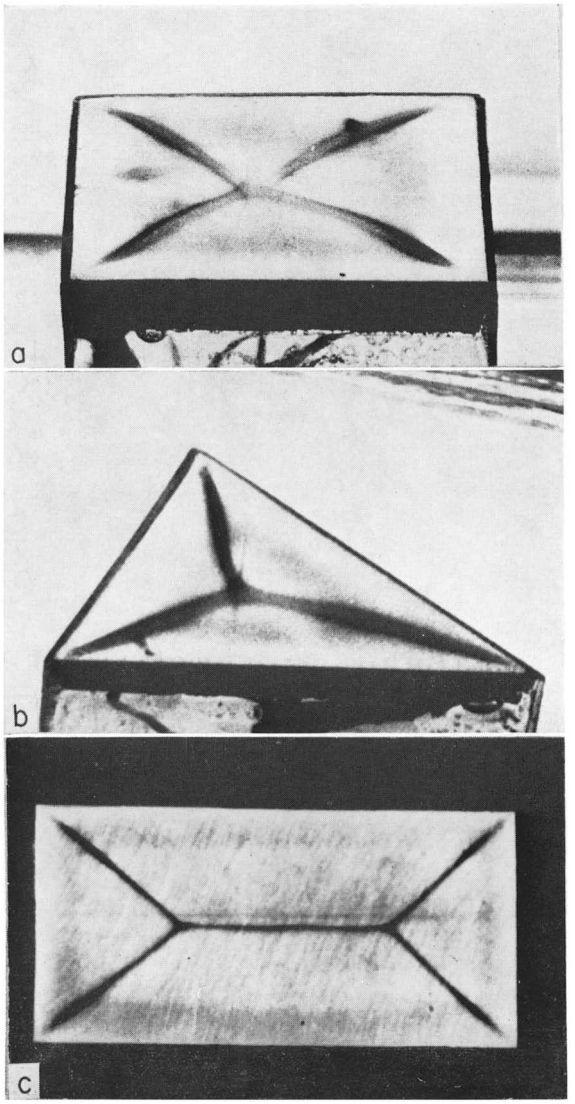

FIG. 1. Partitioning of the flow field ($Gr\ Pr = 2 \times 10^6$).

facing page 1206

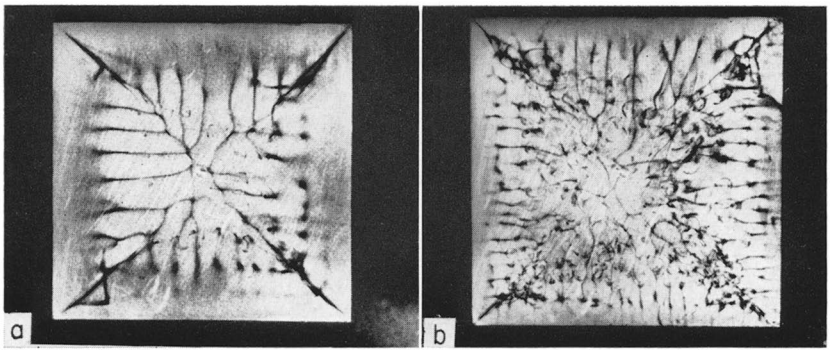

FIG. 2. Flow patterns for surfaces of square planform. (a) $Gr\,Pr = 1{\cdot}5 \times 10^8$. (b) $Gr\,Pr = 5{\cdot}5 \times 10^8$.

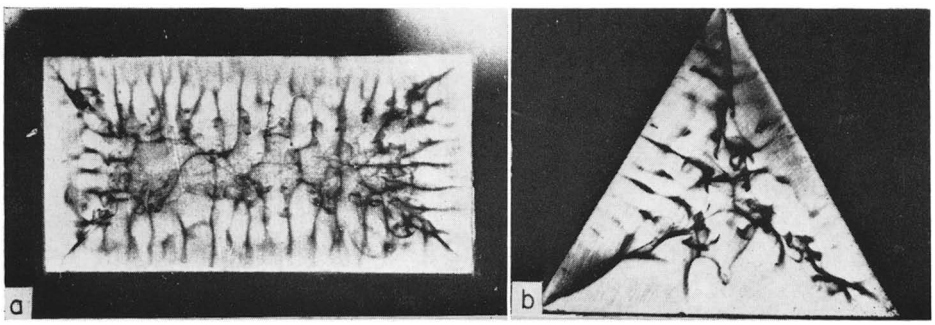

FIG. 3. Flow patterns for surfaces of rectangular and triangular planform. ($Gr\,Pr = 4 \times 10^7$).

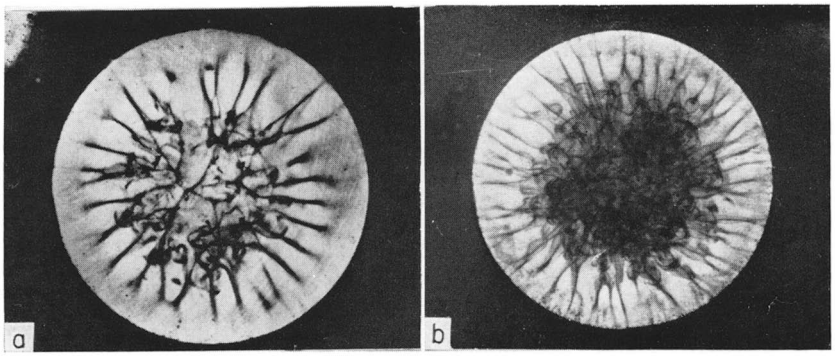

FIG. 4. Flow patterns for surfaces of circular planform. (a) $Gr\,Pr = 10^8$. (b) $Gr\,Pr = 3{\cdot}5 \times 10^8$.

listed in Table 1, which also includes pertinent dimensions. The test specimens were fabricated from copper plate, approximately 0·5-cm thick. Each of the specimens was mounted in a plastic holder. In this arrangement, the test specimen appears to be the top of a table having solid vertical side walls. The side walls are thin plexiglass sheets (thickness = 0·5 mm) cemented to the edges of the test specimen. As a result of this mounting arrangement, the heated test surfaces were positioned about 8 cm above the floor of the test chamber.

Table 1. *Test surfaces*

Surface	Dimensions (cm)
square	5 × 5
square	8·9 × 8·9
rectangle	5·1 × 10·2
equilateral triangle	side = 5·7
circle	diameter = 5
circle	diameter = 8·7

The test chamber was a plexiglass tank 25-cm wide and 31-cm long, filled to a height of approximately 30 cm with distilled water. Thymol blue, a pH indicator, is added to the water in minute amount,* and the solution is titrated to the end point (pH ~ 8) with sodium hydroxide and then made acidic, and yellow in color, by the addition of hydrochloric acid [1]. If a d.c. voltage† is impressed between the test surface (acting as negative electrode) and a copper electrode situated elsewhere in the working fluid, there is a proton transfer reaction at the test surface. As a consequence, there is a change in the pH of the fluid at the surface, with a corresponding change in color from yellow to blue. This process does not give rise to density differences within the fluid, so no extraneous buoyancy forces are induced.

The thus-formed "dye" faithfully follows the motion of the fluid. Pulse-like application of the d.c. voltage favors the observation of the flow field in the immediate neighborhood of the plate, the distracting buoyant plume not being visible. Prolonged application of the d.c. voltage permits observation of the entire flow field, although the billowing plume obscures large portions of the test surface.

Heating of each of the test specimens was accomplished by electrical means, by resistance wire cemented to the downward-facing surface. Specimen temperature was measured by pairs of copper–constantan thermocouples soldered into holes drilled into the down-facing surface. The temperature of the working fluid was read from a precision thermometer. At any given time, only one of the test specimens was situated in the test chamber.

* 0·01 per cent by weight.

† Between 4 and 10 V, depending on the test conditions.

Photographs of the flow patterns were taken with an Exakta camera. In most cases, the camera was situated so that it looked directly down on the test surface from above. Some photos were taken from the side, through the plexiglass side walls of the test chamber. Yellow photoflood lighting was employed to highlight the flow field.

RESULTS

A basic characteristic of free convection flows adjacent to planforms with corners is the partitioning of the flow field. This behavior is illustrated in Fig. 1, for the square, the equilateral triangle, and the 2:1 rectangle. The first two photographs were taken from the side and the last from directly above. As seen in the figure, the partitions very nearly coincide with the bisectors of the angles of the planform. In the case of the rectangle, the central partition is a longitudinal symmetry line. There is no flow across a partition line. Rather, each partition line is a central element of a vertically ascending buoyant plume. The partition lines are created by the interaction of the flows streaming inward along the plate surface from the separate edges. Once granting the existence of the partition lines, the flows in each of the thus-cordoned-off regions of the plate surface may be regarded as more or less independent of each other.

In Fig. 1, as well as in succeeding figures, the Grashof–Prandtl product, $GrPr$, appears as a characterizing parameter. The relevant fluid properties were evaluated at a reference temperature which is the average of the plate and bulk fluid temperatures. The characteristic dimension appearing in the Grashof number was selected as follows: square and equilateral triangle–side, rectangle–short side, circle–diameter.

Details of the flow field for the square plate are shown in Fig. 2. From these photographs, it is seen that within each of the four partitioned-off sections of the plate, the flow moves along parallel paths, each path being more or less perpendicular to the edge of the plate. When the flow approaches the region of the partition lines, it is engulfed in a vertically ascending buoyant plume. The waviness of the flow pattern in the neighborhood of the partition lines is a result of the meandering nature of the rising plume. This is particularly evident in the central region of the plate [Fig. 2(b)]. The flow field in each of the partitioned-off sections of the plate appears to be a mirror image of that in the neighboring sections.

Flow field details for the 2:1 rectangle and equilateral triangle are shown in Fig. 3. The flow paths illustrated therein are of the same nature as those just discussed for the square. Fluid moves inward from the edges along paths that are straight and parallel. Upon reaching the neighborhood of the partition lines, the flow is engulfed in the upward-moving, somewhat-wandering plume. For the rectangle, it appears that, for purposes of analysis, the problem can be decomposed into two sub-problems. One sub-problem

would be that of a square plate made up of the two end sections of the rectangle. The second sub-problem would be that of a strip of infinite length (i.e. without ends).

The flow field characteristics for a circular plate are somewhat different from those of planforms having corners. In particular, as illustrated in Fig. 4, partition lines are absent. While the flow paths are perpendicular to the edges of the plate, they are convergent rather than parallel. The convergence of the paths tends to accelerate the flow as it moves inward toward the center of the plate. The central region of the plate is dominated by a billowing plume.

In the view of the authors, the flow field information suggests that generalization of existing (albeit conflicting) square plate heat-transfer correlations to other planforms may involve more than simply using the short side as the characteristic dimension [4].

ACKNOWLEDGEMENT

The authors gratefully acknowledge the assistance of Janja D. Husar in the execution of the experiments.

REFERENCES

1. D. J. BAKER, A technique for the precise measurement of small fluid velocities, *J. Fluid Mech.* **26**, 573–575 (1966).
2. W. H. MCADAMS, *Heat Transmission*, 3rd edn. McGraw-Hill, New York (1954).
3. M. FISHENDEN and O. A. SAUNDERS, *An Introduction to Heat Transfer*. Clarendon Press, Oxford (1950).
4. M. MIKHEYEV, *Fundamentals of Heat Transfer*. Peace, Moscow.
5. R. C. L. BOSWORTH, *Heat Transfer Phenomena*. John Wiley, New York (1952).
6. R. WEISE, Wärmeübergang durch Freie Konvektion an quadratischen Platten, *Forsch. Geb. IngWes* **6**, 281 (1935).
7. W. KRAUS, Temperatur- und Geschwindigkeitsfeld bei Freier Konvektion um eine waagerechte quadratische Platte, *Phys. Z.* **41**, 126 (1940).

Int. J. Heat Mass Transfer Vol. 11, pp. 1208–1211 Pergamon Press 1968 Printed in Great Britain

BOUNDARY-LAYER ANALYSIS OF THE FLOW BOILING CRISIS

L. S. TONG

Manager of Thermal and Hydraulic Engineering, Atomic Power Divisions, Westinghouse Electric Corporation, Pittsburgh, Pennsylvania, U.S.A.

(*Received* 17 *August* 1967 *and in revised form* 20 *December* 1967)

NOMENCLATURE

B,	$= G^+/(f/2)$;
C,	constant;
D_e,	equivalent diameter [ft];
f,	friction factor;
G,	mass velocity [lb/h ft^2];
H_{fg},	heat of evaporation [Btu/lb];
p,	pressure [lb/in^2];
q'',	heat flux [Btu/h ft^2];
Re,	Reynolds number;
ΔT_{sc},	subcooling [°F];
U_o,	main stream velocity [ft/s];
u,	flow velocity parallel to wall [ft/s];
V,	flow velocity normal to wall [ft/s];
y,	distance normal to wall [ft];
x,	distance parallel to wall [ft].

Greek symbols

α,	void fraction;
δ,	thickness of boundary layer [ft];
ρ,	density [lb/ft^3];
τ,	shear [lb/ft^2];
μ,	viscosity [lb/h ft];
χ,	steam quality.

Subscripts

δ,	refers boundary-layer thickness;
j,	refers injection flow;
l,	refers saturated liquid condition;
L,	refers laminar flow;
M,	refers mixture;
o,	refers main stream properties;
T,	refers turbulent;
TP,	refers two-phase flow;
v,	refers saturated vapor condition;
w,	refers wall condition;
lam,	refers laminar sublayer condition;
sat,	refers saturated condition;
crit,	refers boundary-layer separation condition;
inj,	refers permeable flat plate;
non-inj,	refers non-permeable flat plate.